Anton DEREVYANKO
Sergiy YERSHOV
Podgorny Institute for Mechanical Engineering Problems of NAS of Ukraine,
anton.derevyanko@gmail.com ,yershov@ipmach.kharkov.ua

PREDICTION OF LAMINAR-TURBULENT TRANSITION WITH THE LOW-REYNOLDS MODEL AND KINETIC ENERGY PRODUCTION LIMITER

A bypass transition model has been implemented in the FlowER solver. The model is based on the Shear Stress Transport turbulence model and Low-Reynolds transition model with the kinetic energy production limiter. The modifications of transition model are implemented to enable fully turbulent flow beyond the transition region. Test cases include the classical flat-plate boundary flows and low-pressure compressor cascade. It is shown that proposed model allows an approximate simulation of some effects in a transitional flow.

Key words: turbulence, transition, low-Reynolds model

1. INTRODUCTION

This paper describes the implementation of an engineering transition model in the CFD solver, FlowER. FlowER is the in-house solver which is developed for computing steady and unsteady 3D compressible viscous flows. It is based on solving the Reynolds-Averaged Navier-Stokes (RANS) equations. RANS techniques utilize a turbulence model solving one or two additional transport equations to represent the mean turbulent effect, and universally predicts the onset of transition to occur much too close to the origin of the boundary layer. Most turbulence models don't have explicit mechanism for transition modeling and are only able to simulate that process via a rapid growth of the turbulence production. Often papers, devoted turbulent flows in turbine cascades do not account laminar-turbulent transition, despite the fact that it is important for determining the local peaks of the skin friction, wall temperature and heat transfer.

Engineering transition predictions are based mainly on three modeling concepts. The first is the use of low-Reynolds number turbulence models [2], the second is the use of experimental correlations [1] and the third is to use additional intermittency transport equations (Menter proposed to use two additional transport equations – for intermittency and for momentum thickness Reynolds number [4]). Considered transition-solving method is based on well-known low-Reynolds turbulence model with addition limiter, which corrects turbulence energy production.

2. FLOW MODEL AND NUMERICAL METHOD

We use steady RANS equations with the k-ω SST turbulence model for description of turbulent flow. Function and constants of the model are the same as given in the original Menter's paper [3]. To increase reliability of turbulent flow computations we use additional realisability constraint for turbulent viscosity coefficient:

$$\omega \geq \frac{\sqrt{3}}{2}\sqrt{S^2 - \frac{2}{3}S_{nn}^2}\ . \tag{1}$$

As a result formula for turbulent viscosity coefficient takes the following form

$$\mu_t = \frac{\rho k}{\max\left(\omega, Sf_2/a_1, \frac{\sqrt{3}}{2}\sqrt{S^2 - 2S_{nn}^2/3}\right)}\ . \tag{2}$$

We consider subsonic flow therefore we need to specify four flow parameters at inlet (total temperature and pressure, inlet flow angels) and one at exit (static pressure).

Numerical method is the implicit second order accurate scheme, ENO approach with the minmod limiter. Our solver performs exact solution of the Riemann problem.

3. TRANSITION MODEL

We have considered a number of approaches which are used to calculate transition in the boundary layer. This analysis allowed us to select low-Reynolds model for the implementation into FlowER. This approach has several advantages:

- it is based on locally computed variables only. Whereas using the integral quantities, such as momentum thickness, leads to increasing computational time for complex flows. Moreover, such values cannot be always accurately calculated;
- it requires only minor changes of the original high-Reynolds model;
- it does not require significant grid refinement and hence may be used to calculate flows in turbomachinery.

Shown below equations are low-Reynolds (LR) turbulence model which is based on Menter's k-ω SST:

$$\frac{\partial \rho k}{\partial t}+\frac{\partial}{\partial x_j}\left[\rho u_j k-(\mu+\sigma_k\mu_t)\frac{\partial k}{\partial x_j}\right]=\alpha_{PTM}P_k-\beta\rho\omega k \tag{3}$$

$$\frac{\partial \rho\omega}{\partial t}+\frac{\partial}{\partial x_j}\left[\rho u_j\omega-(\mu+\sigma_\omega\mu_t)\frac{\partial \omega}{\partial x_j}\right]= \\ \frac{\alpha\rho}{\mu_t}P_k-\beta\rho\omega^2+(1-F_1)\rho\sigma_{\omega 2}\frac{1}{\omega}\frac{\partial k}{\partial x_j}\frac{\partial \omega}{\partial x_j}, \tag{4}$$

where ρ is density, k is turbulent kinetic energy, ω is specific dissipation rate, μ is dynamic molecular viscosity, μ_t is dynamic turbulent viscosity, $P_k=\tau_{tij}S_{ij}$ is production of turbulent kinetic energy (TKE), τ_{tij} is Reynolds-stress tensor, S_{ij} is averaged strain-rate tensor, σ_k, β, σ_ω, α, β are constants.

The F_1 and F_2 are switching functions, which activates k-ω model near the wall boundaries and switches the model to k-ε away from the walls:

$$F_1=\max(\mathrm{th}(arg_1^4);\exp(-(R_y/120)^8))$$
$$arg_1=\min\left(\max\left(\frac{\sqrt{k}}{\beta^*\omega y};\frac{500\mu}{\rho\omega y^2}\right);\frac{4\rho\sigma_{\omega 2}k}{CD_{k\omega}y^2}\right)$$
$$CD_{k\omega}=\max\left(2\rho\sigma_{\omega 2}\frac{1}{\omega}\frac{\partial k}{\partial x_j}\frac{\partial \omega}{\partial x_j};10^{-20}\right)$$
$$\mu_t=\min\left(\alpha^*\frac{\rho k}{\omega};\frac{0{,}31\rho k}{SF_2}\right) \tag{5}$$
$$S=\sqrt{2S_{ij}S_{ij}}\ ,\ F_2=\mathrm{th}(arg_2)$$
$$arg_2=\min\left(2\frac{\sqrt{k}}{\beta^*\omega y};\frac{500\mu}{\rho\omega y^2}\right)$$

where y distance to nearest solid boundary in the flow, $R_y=\rho y\sqrt{k}/\mu$ turbulent Reynolds number based on wall distance.

Production Term Modifier α_{PTM} corrects TKE production at non-turbulent and transitional region. It is used to control the transition onset location:

$$\alpha_{PTM} = 1 - 0.94 P(Re_v) F_3 \mathrm{th}((y^+/17)^2), \quad (6)$$

where P is the function that depends on viscosity-based Reynolds number $Re_v = y^2 S / \nu$. Function F_3 depends on turbulent Reynolds number R_y. Multiplier $\mathrm{th}((y^+/17)^2)$ is added to turn off α_{PTM} limiter in turbulent part of boundary layer, where $y^+ = y u_\tau / \nu$ is dimensionless distance from a wall, $u_\tau = \sqrt{\tau_w / \rho_w}$ is friction velocity, τ_w and ρ_w are stress tensor and density, calculated at a wall.

4. TEST CASES

First computations were performed on a zero-pressure gradient flat plate. There are experimental results for such type of flows in the ERCOFTAC database. Three experiments with different inlet turbulence intensity were chosen for model testing.

Table 1. Test cases experimental conditions

Test case	Flow velocity, m/s	Turbulence intensity, %
T3A	5,4	3,0
T3B	9,4	6,0
T3A-	19,8	0,9

Parameters are chosen in such a way to provide different onset positions. It placed at a plate leading edge in T3B experiment, at the plate center in T3A and in the end of plate for T3A- test case.

Computational domain has 120 cells in streamwise direction and 80 cells in crosswise direction. Grid refinement near plate surface insures a y+ value to be less than 1. FlowER intended to calculate flows in the turbine and compressor cascades. These tests were conducted at extremely low flow velocities. The calculation of such flows in FlowER requires more computation time and subjected to additional inaccuracies.

The skin friction distributions for all experiments are displayed in fig. 1-3. As expected, the original high-Reynolds k-ω SST turbulence model (market as HR on the plot) overestimates value of turbulence intensity, and predicts transition to turbulent boundary layer at leading edge of the plate for all three tests. The LR k-ω SST model without additional turbulence production limiter allows determining transition onset, but has several drawbacks: it underestimates value of turbulence intensity behind transitional region, where boundary layer is completely turbulent, and not computes transition for the T3A- test case at all.

The LR model with PTM limiter (LR-PTM) describes transition better and works well for the T3A- test.

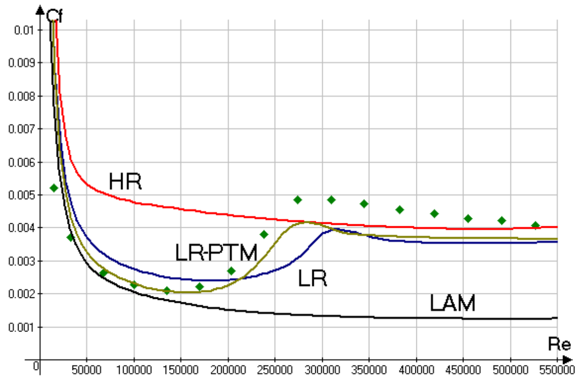

Fig. 1 Skin friction – T3A test case

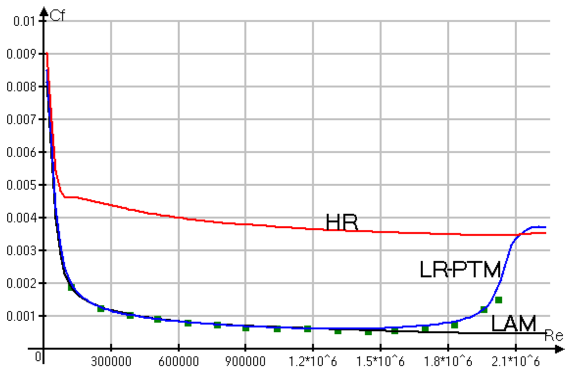

Fig. 2 Skin friction – T3A- test case

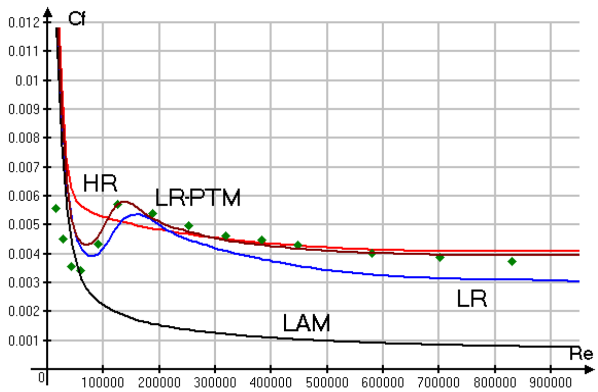

Fig. 3 Skin friction – T3B test case

The further model verification was performed with the experimental data for transitional gas flow in a compressor channel [5]. The experiment was performed under the following conditions:

- inlet flow speed – 32.88 m/s;
- inlet total pressure – 101.6 kPa;
- outlet static pressure – 101.3 kPa;
- inlet turbulence free stream intensity – 0.18%.

Computational domain has 120 cells circumferential, 96 cells in radial and 180 in streamwise directions (total number ≈ 2 million). Grid refinement near solid borders insures a y+ value to be approximately 1.

Figures 4-5 shows the TKE distribution around the blade, obtained using the original HR k-ω SST and the LR-PTM models. We can find again that the original HR k-ω SST model forces transition to appear near leading edge of the blade. Turbulence kinetic energy increases rapidly in the small separation bubble and remains high in boundary layer throughout the length of the blade. On the pressure side onset is shifted downstream, but still located close to the leading edge.

The LR-PTM model shows another turbulent kinetic energy distribution: it decreases maximum value of TKE; transition region is shifted downstream to the middle of blade-chord for the suction side. Boundary layer on the pressure side remains laminar along whole plate.

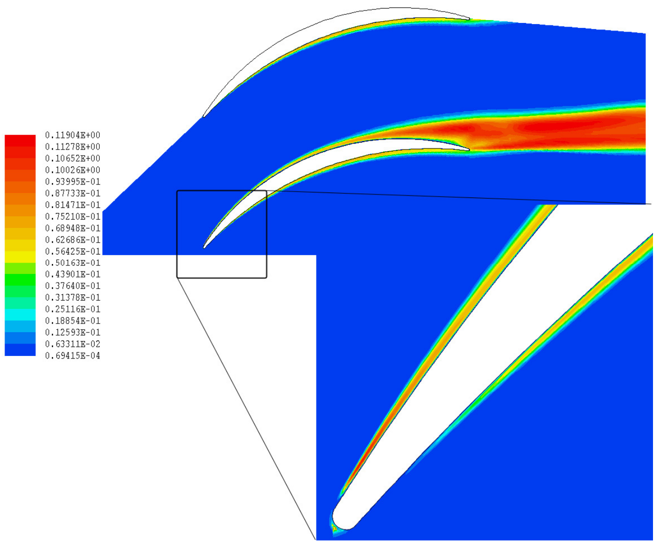

Fig. 4 Turbulence intensity – high-Reynolds model

Fig. 6 shows the streamwise distribution of skin friction coefficient. Experimental data shows that there are several zones of increased and decreased C_f value at suction side. That seems to indicate flow type changing. It is seen that the HR model accurately describes the turbulent part of the flow on the suction side, but it does not take into account fluctuations of skin friction in relaminarization regions. The distribution differs significantly from the experimental data on the pressure side due to turbulence kinetic energy overestimation.

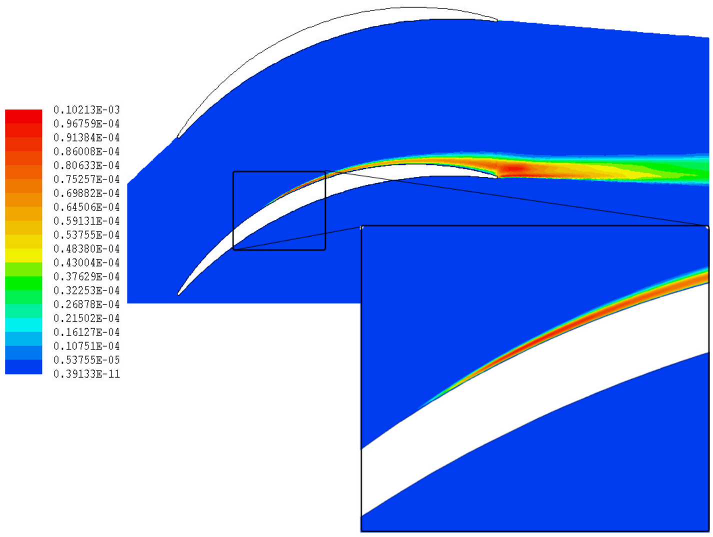

Fig. 5 Turbulence intensity – LR-PTM model

The LR-PTM model qualitatively reflects the C_f plot changings, although the magnitude deviates from the experimental data. Skin friction data are much closer to the experimental on the pressure side than for the original HR model.

5. CONCLUSIONS

The laminar-to-turbulent transition model has been implemented and validated in the FlowER solver. The model is intended for flows where bypass transition is the dominant laminar-to-turbulent transition mechanism. It is shown that model with the production term modifier better describes turbulent production downstream of the transition location compared to original low-Reynolds turbulent number model. Further, it accomplishes this without the expense of adding any additional transport equations or requiring calculation of integrated parameters such as momentum thickness. It reproduces transition onset accurately in zero pressure gradient test cases. Calculations of gas flow in compressor cascade were also performed. Results showed qualitative agreement with experimental data However skin friction value in the transitional zone is significantly different in experiment and calculation. We plan further model testing for the flows in the turbine cascade on which we will perform adjustment and tuning the proposed method.

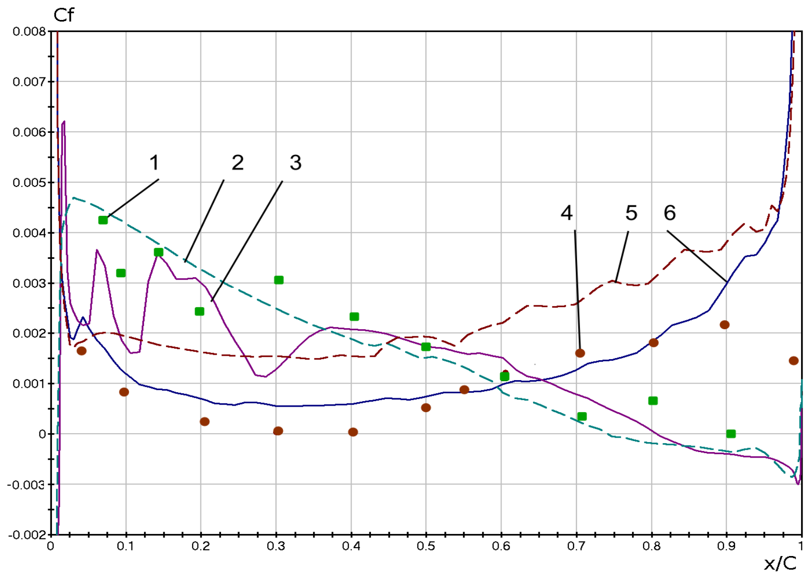

1. Suction side, experimental data;
2. Suction side, HR k-ω SST Menters;
3. Suction side, LR-PTM;
4. Pressure side, experimental data;
5. Pressure side, HR k-ω SST Menters;
6. Pressure side, LR-PTM.

Fig. 6 Skin friction distribution

REFERENCES

[1] Abu-Ghannam, B.J., and Shaw, R., 1980, *Natural Transition of Boundary Layers – The Effects of Turbulence, Pressure Gradient, and Flow History*, J. Mech. Eng. Sci., 22(5), pp. 213-228.

[2] Jones, W.P. and Launder, B.E., 1972, *The prediction of lamirazation with a two-equation model of turbulence*. International Journal of Heat and Mass Transfer, 15, pp. 301-314.

[3] Menter, F.R. 1994, *Two-Equation Eddy-Viscosity Turbulence Models for Engineering Applications*. AIAA J.32, No 8. pp. 1598 – 1605.

[4] Menter, F.R., Langtry, R.B., Likki, S.R., Suzen, Y.B., Huang, P.G., and Völker, S., 2004, *A Correlation Based Transition Model Using Local Variables Part I-Model Formulation*, Vienna, ASME Paper No. ASME-GT2004-53452.

[5] Zierke, W.C. Steven Deutsch, 1989, *The Measurement of Boundary Layers on a Compressor Blade in Cascade*, NASA Contractor Report 185118, – 1989. – P. 226